Acta Crystallographica Section F
Structural Biology and Crystallization Communications
ISSN 1744-3091

Structure of the SH3 domain of human osteoclast-stimulating factor at atomic resolution

Liqing Chen,[a,b,c]* Yujun Wang,[a,b,c] David Wells,[a] Diana Toh,[a] Hunt Harold,[a] Jing Zhou,[a,b,c] Enrico DiGiammarino[a] and Edward J. Meehan[a,b,c]

[a]Laboratory for Structural Biology, University of Alabama in Huntsville, Huntsville, Alabama 35899, USA, [b]Department of Chemistry, University of Alabama in Huntsville, Huntsville, Alabama 35899, USA, and [c]Graduate Program of Biotechnology, University of Alabama in Huntsville, Huntsville, Alabama 35899, USA

Correspondence e-mail: chenlq@uah.edu

Received 18 April 2006
Accepted 31 July 2006

PDB Reference: osteoclast-stimulating factor, 1zlm, r1zlmsf.

Osteoclast-stimulating factor (OSF) is an intracellular signaling protein, produced by osteoclasts themselves, that enhances osteoclast formation and bone resorption. It is thought to act *via* an Src-related signaling pathway and contains SH3 and ankyrin-repeat domains which are involved in protein–protein interactions. As part of a structure-based anti-bone-loss drug-design program, the atomic resolution X-ray structure of the recombinant human OSF SH3 domain (hOSF-SH3) has been determined. The domain, residues 12–72, yielded crystals that diffracted to the ultrahigh resolution of 1.07 Å. The overall structure shows a characteristic SH3 fold consisting of two perpendicular β-sheets that form a β-barrel. Structure-based sequence alignment reveals that the putative proline-rich peptide-binding site of hOSF-SH3 consists of (i) residues that are highly conserved in the SH3-domain family, including residues Tyr21, Phe23, Trp49, Pro62, Asn64 and Tyr65, and (ii) residues that are less conserved and/or even specific to hOSF, including Thr22, Arg26, Thr27, Glu30, Asp46, Thr47, Asn48 and Leu60, which might be key to designing specific inhibitors for hOSF to fight osteoporosis and related bone-loss diseases. There are a total of 13 well defined water molecules forming hydrogen bonds with the above residues in and around the peptide-binding pocket. Some of those water molecules might be important for drug-design approaches. The hOSF-SH3 structure at atomic resolution provides an accurate framework for structure-based design of its inhibitors.

1. Introduction

The osteoclast (OCL) is the primary bone-resorbing cell responsible for degradation of bone matrix (Roodman, 1996). Factors produced by OCL play an important role in regulating OCL formation and activity (Reddy & Roodman, 1998). A novel 28 kDa intracellular protein termed osteoclast-stimulating factor (OSF), highly expressed in OCL, indirectly enhances OCL formation and bone resorption through a cellular signal transduction cascade, possibly through its interaction with c-Src or other c-Src-related proteins (Reddy *et al.*, 1998). OSF contains a short proline-rich N-terminal region, an SH3 domain, three ankyrin repeats and an aspartate-rich C-terminal region (Reddy *et al.*, 1998), suggesting that it is potentially involved in protein–protein interactions. Its SH3 domain was found to interact with the 40 kDa spinal muscular atrophy disease-determining gene product, survival motor neuron (SMN), to stimulate OCL formation (Kurihara *et al.*, 2001), indicating that OSF SH3–SMN interaction may play an important role in congenital bone fractures associated with type I spinal muscular atrophy disease. Inhibition of the interaction of the OSF-SH3 domain with its protein partners might lead to reduced bone resorption by OCL and thus prevent the bone loss that is associated with many bone diseases, such as periodontal disease, osteoporosis, estrogen deficiency, Paget's disease, inflammatory bone loss, bone malignancy and hyperparathyroidism.

As part of a structure-based anti-bone-loss drug-design program, we have determined a high-resolution X-ray structure of the recombinant human OSF SH3 domain (hOSF-SH3). The structure provides an accurate framework for structure-based studies of SH3-domain inhibitors.

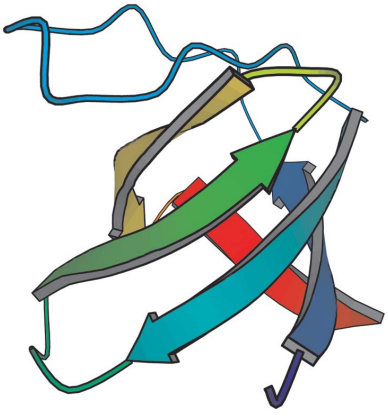

2. Materials and methods

2.1. Cloning and expression

The gene for hOSF (GenBank accession No. NM_012383) was obtained from OpenBiosystem's IMAGE clone collection (ID BC007459). A truncated fragment of OSF coding for residues 12–72 (SH3 domain) was PCR subcloned using primers 5′-GACAGC-TAGCGGGCAAGTTAAAGTCTTCAGAGC-3′ and 5′-CGCGGAT-CCTTAGGATTCTGCCTGCTCAGCCAC-3′ into the *Nhe*I/*Bam*HI restriction sites of pET28b (Novagen). The pET28-OSF-SH3 vector containing a six-His tag was transformed into *Escherichia coli* BL21(DE3) (Novagen) and the overproduction of the protein was induced at an $A_{600\,nm}$ of ∼1.0 with a final concentration of 1 m*M* IPTG at 291 K. The cells grew for an additional 12 h and were harvested by centrifugation and frozen at 253 K.

2.2. Protein purification

The cell pellet was resuspended in Ni buffer *A* (20 m*M* Tris pH 8.0, 500 m*M* NaCl, 5 m*M* imidazole), lysed by sonication and centrifuged at 20 000*g* for 20 min at 277 K. The soluble crude lysate was filtered through a 0.45 µm filter and applied onto a Chelating Sepharose column (Pharmacia) which had been previously charged with 50 m*M* $NiSO_4$ and equilibrated with Ni buffer *A*. The column was then washed with Ni buffer *A* to remove unbound proteins. The His_6-SH3 fusion protein was eluted with a 5–500 m*M* imidazole linear gradient in 20 m*M* Tris–HCl pH 8.0, 500 m*M* NaCl and then dialyzed against high-salt thrombin cleavage buffer (20 m*M* Tris–HCl pH 8.4, 500 m*M* NaCl, 2.5 m*M* $CaCl_2$) overnight at 277 K. One unit of thrombin protease (Novagen) was added per milligram of fusion protein and the His tag was cleaved for 4 h at room temperature. The thrombin cleavage reaction was terminated by a 1:10 dilution with 20 m*M* Tris–HCl pH 8.0 and the mixture was applied onto a Q Sepharose column (Pharmacia) that had been previously equilibrated with Q buffer *A* (20 m*M* Tris–HCl pH 8.0, 50 m*M* NaCl). SH3 was eluted from Q Sephrose with a 50–1000 m*M* NaCl linear gradient in 20 m*M* Tris–HCl pH 8.0. Fractions containing SH3 were pooled and concentrated by ultrafiltration.

2.3. Crystallization and data collection

The stock protein solution used for crystallization contained 20 m*M* Tris–HCl buffer pH 8.0 and 200 m*M* sodium chloride with a protein concentration of 10 mg ml^{-1}. Crystals were grown at 277 K by the sitting-drop vapor-diffusion method with 100 m*M* sodium HEPES buffer pH 7.5, 2%(*v*/*v*) polyethylene glycol (PEG) 400, 2 *M* ammonium sulfate as the reservoir solution. The crystallization drops were prepared by mixing 5 µl protein solution with 4 µl reservoir solution and were equilibrated against 500 µl reservoir solution. Useful crystals appeared within a week and grew to a typical size of about 0.15 × 0.07 × 0.03 mm. Crystals formed in space group $C222_1$, with unit-cell parameters a = 36.81, b = 80.48, c = 49.16 Å, and contained one monomer in the asymmetric cell. X-ray diffraction data to 1.07 Å resolution were collected at beamline 22-ID in the facilities of the South East Regional Collaborative Access Team (SER-CAT) at the Advanced Photon Source, Argonne National Laboratory, USA. The program package *HKL*-2000 was used to process the diffraction data (Otwinowski & Minor, 1997). The statistics for data collection and processing are summarized in Table 1.

2.4. Structure determination and refinement

The orientation and position of hOSF-SH3 in the crystal unit cell were determined using the molecular-replacement protocols in the program *CNS* (Brünger *et al.*, 1998) with the structure of Grb2 (PDB code 1gri) as the search model. The composite OMIT map was calculated to guide electron-density fitting of the model. Energy-restrained crystallographic refinement was carried out with the maximum-likelihood algorithms implemented in *CNS*. Refinement proceeded through several cycles in combination with manual checking with the program *O* (Jones *et al.*, 1991). The addition of 100 water molecules and refinement to 1.07 Å resulted in R and R_{free} values of 0.243 and 0.245, respectively. Further refinement was continued with *SHELX*97 (Sheldrick & Schneider, 1997), first subjecting the structure to cycles of isotropic conjugate-gradient least-squares refinement; tightly restrained anisotropic displacement parameters were then introduced and refined. No bulk-solvent model (*SHELXL* SWAT option) was used during the refinement as it did not substantially lower the R factors. The final refinement cycle resulted in R and R_{free} values of 0.158 and 0.211, respectively. The final model contains residues 12–69 and 130 water molecules. The phasing and refinement statistics are summarized in Table 1.

Table 1
Summary of data collection, phasing and refinement.

Values in parentheses are for the highest resolution shell.

Data and phasing statistics	
Space group	$C222_1$
Unit-cell parameters (Å)	a = 36.81, b = 80.48, c = 49.16
Wavelength (Å)	1.00
Resolution (Å)	1.07 (1.11–1.07)
Wilson B factor (Å^2)	9.5
Reflections (total/unique)	142748/28252
Completeness (%)	86.3 (49.9)
$I/\sigma(I)$	17.4 (2.5)
$R_{merge}(I)$ (%)	9.8 (24.1)
Molecular-replacement model	Grb2 SH3 domain
Refinement statistics	
Resolution range (Å)	10–1.07
No. of reflections	27365
No. of atoms	
Protein	477
Water	130
R factors	
R_{work} (%)	15.8
R_{free} (%)	21.1
R.m.s. deviation of bonds	
Lengths (Å)	0.014
Angle distances (°)	0.030
Average B factor (Å^2)	20.8

2.5. Protein-fold analysis

Secondary-structure elements were defined by the hydrogen-bonding patterns in combination with visual inspection. The *DALI* algorithm of comparing protein domain structures by alignment of distance matrices was used to search for structural homologs of the hOSF-SH3 domain and was also used for structure-based sequence alignment (Holm & Sander, 1993, 1998). Ribbon diagrams were prepared using the program *MOLSCRIPT* (Kraulis, 1991).

3. Results and discussion

3.1. Structure determination

The hOSF-SH3 domain included residues 12–72 of the hOSF sequence (Reddy *et al.*, 1998). hOSF-SH3 was crystallized and its structure was determined by the molecular-replacement method (Table 1). The structure was refined against 1.07 Å resolution data, making it one of the highest resolution SH3-domain structures reported to date (Berisio *et al.*, 2001; Wisniewska *et al.*, 2005; Hoelz *et al.*, 2006). The C-terminal residues 70–72 were disordered and could

Table 2
Alignment statistics of hOSF-SH3 with structurally similar SH3 domains.

Produced by the *DALI* algorithm (Holm & Sander, 1993, 1998).

Protein	PDB code	*Z*†	R.m.s.d.‡ (Å)	LALI§	LSEQ2¶	IDE†† (%)	Reference
hOSF-SH3 domain	1zlm	15.3	0.0	58	58	100	This paper
Oncogene c-Crk	1cka	11.4	1.0	55	56	33	Wu *et al.* (1995)
Neutrophil cytocol factor 4	1w6x	11.1	1.0	54	56	31	Massenet *et al.* (2005)
Tyrosine kinase Lck	1lck	10.8	1.0	54	164	37	Eck *et al.* (1994)
Actin-binding protein Abp1	1jo8	10.5	1.0	54	58	37	Fazi *et al.* (2002)
Signal transduction adaptor Grb2	1gri	10.0	0.7	54	211	44	Maignan *et al.* (1995)
Tyrosine kinase Abl	1bbz	9.7	1.4	54	58	26	Pisabarro *et al.* (1998)
Anti-oncogene 53BP2	1ycs	9.6	1.2	55	193	31	Gorina & Pavletich (1996)
Tyrosine kinase c-Src	1fmk	9.6	1.4	55	438	44	Xu *et al.* (1997)

† *Z* score, strength of structural similarity in standard deviations above expected. ‡ Positional root-mean-square deviation of superimposed C^{α} atoms. § Total number of equivalent residues. ¶ Length of the entire chain of the equivalent structure. †† Percentage sequence identity over equivalent positions.

not be seen in the $2F_o - F_c$ electron-density map. The final refined model, which includes residues 12–69 and 130 ordered water molecules, has a working *R* value of 0.158 and a free *R* value of 0.211. The stereochemistry is excellent, with r.m.s. deviations for bond lengths and angle distances of 0.014 and 0.030 Å, respectively (Table 1). The Ramachandran plot statistics showed that 95.9% of the backbone dihedral angles were in most favored regions, 4.1% were in additional allowed regions and none of the non-glycine residues were in disallowed regions.

3.2. Overall structure

Like the structures of other SH3 domains, hOSF-SH3 adopts a classical SH3 fold consisting of five antiparallel β-strands arranged as two orthogonal β-sheets that form a β-barrel (Fig. 1). Each β-sheet consists of three β-strands with one long strand (B2; residues 37–44) contributing different segments to each sheet. One of the sheets is formed by β-strands B2, B1 (residues 14–20) and B5 (residues 65–69), while the other is formed by B2, B3 (residues 48–54) and B4 (residues 57–63). The first two β-strands (B1 and B2) are linked by the RT loop (residues 21–36, named for the RT residues found in the c-Src SH3 domain), which forms a hairpin-like structure. The second β-strand B2 is linked to the third β-strand B3 by a short n-Src loop (residues 45–47). The third loop, linking β-strands B3 and B4, is known as the distal loop (residues 55–56). Residue Asn64 links the last two β-strands B4 and B5.

3.3. Structure comparison and the putative peptide-binding site

The overall structure of hOSF-SH3 is very similar to several other SH3 domains despite having a relatively low sequence homology (Table 2). Among these, hOSF-SH3 has the highest sequence identity with the SH3 domains of signal transduction adaptor Grb2 (44% over 54 equivalent positions) and tyrosine kinase c-Src (44% over 55

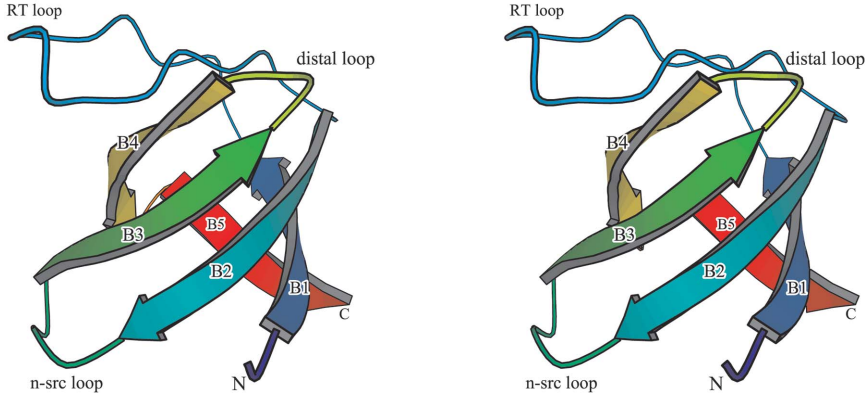

Figure 1
Stereo ribbon representation of the hOSF-SH3 structure. A rainbow ramp color coding of blue to red is used to mimic the chain trace from the N-terminus to the C-terminus. Both termini and the secondary-structure elements are labeled. Positions of the loops are also indicated.

```
1fmk   82 MVTTFVALYDYESRTETDLSFKKGERLQIVNNT   EGDWWLAHSLSTGQTGYIPSNYVAPSDS 142
1ycs  460  KGVIYALWDYEPQNDDELPMKEGDCMTIIHREDEDEIEWWWARL  NDKEGYVPRNLLGLYP  519
1bbz    1   NLFVALYDFVASGDNTLSITKGEKLRVLGYNH  NGEWCEAQT  KNGQGWVPSNYITPVNS  58
1gri  158  PTYVQALFDFDPQEDGELGFRRGDFIHVMDNS   DPNWWKGAC  HGQTGMFPRNYVTPV   213
1jo8    1   PWATAEYDYDAAEDNELTFVENDKIINIEFV   DDDWWLGELEKDGSKGLFPSNYVSLGN   58
1lck   63  DNLVIALHSYEPSHDGDLGFEKGEQLRILEQ    SGEWWKAQSLTTGQEGFIPFNFVAKA   119
1w6x  173   MRAEALFDFTGNSKLELNFKAGDVIFLLSRI   NKDWLEGTV  RGATGIFPLSFVKILY  228
1cka  134  AEYVRALFDFNGNDEEDLPFKKGDILRIRDKP   EEQWWNAED SEGKRGMIPVPYVEKY   190
1zlm   12GQVKVFRALYTFEPRTPDELYFEEGDIIYITDMS   DTNWWKGTS  KGRTGLIPSNYVAEQAES 72
             B1   * *                B2        * B3       B4 * ** B5
```

Figure 2
Structure-based sequence alignment of hOSF-SH3 with the most similar SH3 domains. The sequence numbers for the first and the last residues are indicated. The positions of the β-strands in hOSF-SH3 are indicated by underlining the sequence and are labeled. Residues that are highly conserved in the SH3-domain family are indicated in bold type. Residues that are known to form the proline-rich ligand-binding pocket are marked with an asterisk. See Table 2 for protein PDB codes and references.

Table 3
Hydrogen bonds between OSF and water molecules in the peptide-binding site.

OSF atom	Water atom	Hydrogen-bond distance (Å)
Thr22 N	105 O	2.83
Thr22 O	115 O	2.69
Thr27 OG1	108 O	2.71
Asp46 OD1	138 O	2.40
Asp46 OD2	127 O	2.77
Asp46 OD2	133 O	2.71
Asp46 OD2	138 O	2.98
Thr47 N	128 O	2.91
Asn48 O	123 O	2.87
Asn48 OD1	150 O	2.69
Asn64 O	110 O	2.67
Asn64 OD1	123 O	2.92
Asn64 OD1	140 O	2.51
Asn64 ND2	140 O	2.93
Tyr65 OH	109 O	2.60
Tyr65 OH	137 O	2.79

equivalent positions). The structural similarity Z scores (Holm & Sander, 1993, 1998) range from 11.4 to 9.6, with r.m.s. deviations of equivalent positions in the range 0.7–1.4 Å. Structure-based sequence alignment of these SH3 domains reveals that the putative proline-rich peptide-binding site of hOSF-SH3 consists of residues that are highly conserved in the SH3-domain family (Figs. 2 and 3), including residues Tyr21, Phe23, Trp49, Pro62, Asn64 and Tyr65. Tyr21 and Phe23 come from the RT loop, Trp49 from the β-strand B3, Pro62 from the β-strand B4 and Tyr65 from the β-strand B5, while Asn64 links the β-strands B4 and B5. These residues form the hydrophobic binding pocket. In addition, residues that are less conserved and/or even specific to hOSF are also part of the peptide-binding site (Fig. 4), including residues Thr22, Arg26, Thr27, Glu30, Asp46, Thr47, Asn48 and Leu60, which might be key to designing specific inhibitors for hOSF SH3 domain to fight osteoporosis and related bone-loss diseases.

There are a total of 13 well defined water molecules forming hydrogen bonds with the hOSF SH3 residues in and around the peptide-binding pocket (Table 3; Fig. 4). Six of those water molecules, 105, 115, 109, 137, 140 and 123, form a long water channel along one end of the binding pocket consisting of hOSF residues Tyr21, Thr22, Phe23, Arg26, Asn48, Trp49, Pro62, Asn64 and Tyr65. Four other water molecules, 127, 128, 133 and 138, form another water network at the other end of the binding pocket consisting of residues Asp46, Thr47, Asn48 and Trp49. Some of those water molecules might be important for drug-design approaches.

Recently, an ensemble of 20 NMR structures of hOSF-SH3 was deposited in the Protein Data Bank (PDB code 1x2k). The solution structures have essentially the same arrangement of secondary structure as the X-ray-determined structure reported here, with an overall r.m.s. deviation of around 0.73 Å over 55 equivalent C^{α} positions (residues 15–69).

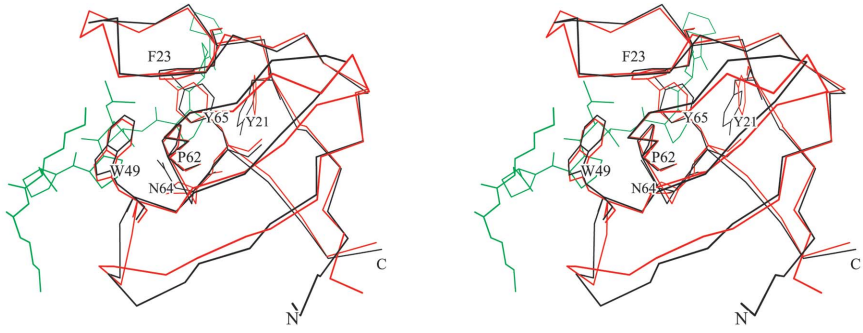

Figure 3
Structure comparison and the peptide-binding model. Stereoview of structural superposition of hOSF-SH3 (black) with c-Crk-SH3 (red; PDB code 1cka) in complex with the proline-rich peptide PPPALPPKK (green). Residues involved in peptide binding are shown as stick models and the rest as C^{α} traces. The peptide is also shown with stick models. For clarity, only the termini and the key residues of hOSF-SH3 are labeled.

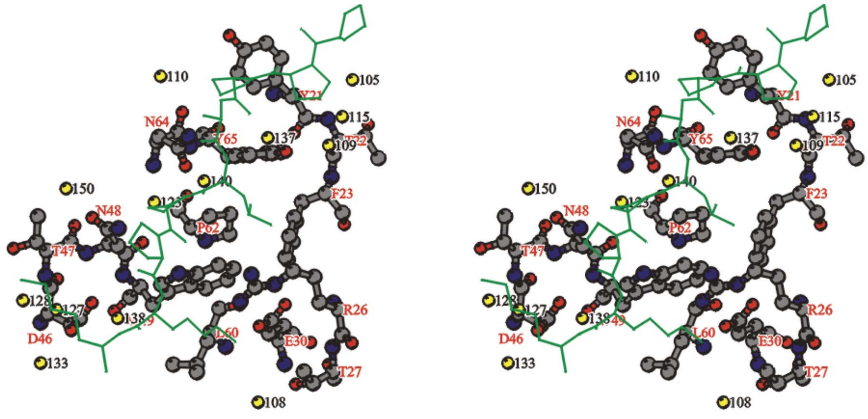

Figure 4
Stereoview of the peptide-binding site showing the water network in and around the binding pocket. To help define the binding pocket, a proline-rich peptide PPPALPPKK (green) was modeled into the proposed peptide-binding site. Residues of hOSF-SH3 forming the peptide-binding pocket are shown as ball-and-stick models and their atoms are colored according to atom types: C atoms, grey; N atoms, blue; O atoms, red. The peptide is shown as a thin-stick model. Water molecules are shown as yellow balls and labeled with black numbers.

3.4. Implications for inhibitor design against osteoclast-mediated bone resorption

OSF induces OCL formation and bone resorption through a cellular signal transduction cascade, possibly through its interactions with c-Src or other Src-related proteins (Reddy *et al.*, 1998). Like the SH3 domains of other proteins, the SH3 domain of hOSF contains a peptide-binding pocket that is also likely to favor the binding of short proline-rich regions in the ligand proteins (Figs. 3 and 4). We are currently working on cocrystallizing the hOSF SH3 domain with proline-rich peptides. Blocking the binding of proline-rich motifs to the pocket of the SH3 domain might disrupt the interactions of hOSF with its signal transduction partners, leading to the inhibition of osteoclast-mediated bone resorption. The atomic resolution crystal structure of hOSF-SH3 as reported here provides an accurate framework for structure-based design of effective SH3-domain inhibitors that might become potential anti-bone-loss drugs.

This work was supported in part by NSF-EPSCoR, NASA and a generous gift from an anonymous donor to the Laboratory for Structural Biology, University of Alabama in Huntsville. Use of the Advanced Photon Source was supported by the US Department of Energy, Office of Science, Office of Basic Energy Sciences under contract No. W-31-109-Eng-38. We thank J. Looger of UAH for technical assistance in computer programs and staff of the SER-CAT beamline 22-ID at the Advanced Photon Source for help with data collection. We are also grateful to OpenBiosystems Inc. for the free gift of hOSF cDNA.

References

Berisio, R., Viguera, A., Serrano, L. & Wilmanns, M. (2001). *Acta Cryst.* D**57**, 337–340.

Brünger, A. T., Adams, P. D., Clore, G. M., DeLano, W. L., Gros, P., Grosse-Kunstleve, R. W., Jiang, J.-S., Kuszewski, J., Nilges, M., Pannu, N. S., Read, R. J., Rice, L. M., Simonson, T. & Warren, G. L. (1998). *Acta Cryst.* D**54**, 905–921.

Eck, M. J., Atwell, S. K., Shoelson, S. E. & Harrison, S. C. (1994). *Nature (London)*, **368**, 764–769.

Fazi, B., Cope, M. J., Douangamath, A., Ferracuti, S., Schirwitz, K., Zucconi, A., Drubin, D. G., Wilmanns, M., Cesareni, G. & Castagnoli, L. (2002). *J. Biol. Chem.* **277**, 5290–5298.

Gorina, S. & Pavletich, N. P. (1996). *Science*, **274**, 1001–1005.

Hoelz, A., Janz, J. M., Lawrie, S. D., Corwin, B., Lee, A. & Sakmar, T. P. (2006). *J. Mol. Biol.* **358**, 509–522.

Holm, L. & Sander, C. (1993). *J. Mol. Biol.* **233**, 123–138.

Holm, L. & Sander, C. (1998). *Proteins*, **33**, 88–96.

Jones, T. A., Zou, J.-Y., Cowan, S. W. & Kjeldgaard, M. (1991). *Acta Cryst.* A**47**, 110–119.

Kraulis, P. J. (1991). *J. Appl. Cryst.* **24**, 946–950.

Kurihara, N., Menaa, C., Maeda, H., Haile, D. J. & Reddy, S. V. (2001). *J. Biol. Chem.* **276**, 41035–41039.

Maignan, S., Guilloteau, J. P., Fromage, N., Arnoux, B., Becquart, J. & Ducruix, A. (1995). *Science*, **268**, 291–293.

Massenet, C., Chenavas, S., Cohen-Addad, C., Dagher, M. C., Brandolin, G., Pebay-Peyroula, E. & Fieschi, F. (2005). *J. Biol. Chem.* **280**, 13752–13761.

Otwinowski, Z. & Minor, W. (1997). *Methods Enzymol.* **276**, 307–326.

Pisabarro, M. T., Serrano, L. & Wilmanns, M. (1998). *J. Mol. Biol.* **281**, 513–521.

Reddy, S., Devlin, R., Menaa, C., Nishimura, R., Choi, S. J., Dallas, M., Yoneda, T. & Roodman, G. D. (1998). *J. Cell. Physiol.* **177**, 636–645.

Reddy, S. V. & Roodman, G. D. (1998). *Crit. Rev. Eukaryot. Gene Expr.* **8**, 1–17.

Roodman, G. D. (1996). *Endocr. Rev.* **17**, 308–332.

Sheldrick, G. M. & Schneider, T. R. (1997). *Methods Enzymol.* **227**, 319–343.

Wisniewska, M., Bossenmaier, B., Georges, G., Hesse, F., Dangl, M., Kunkele, K. P., Ioannidis, I., Huber, R. & Engh, R. A. (2005). *J. Mol. Biol.* **347**, 1005–1014.

Wu, X., Knudsen, B., Feller, S. M., Zheng, J., Sali, A., Cowburn, D., Hanafusa, H. & Kuriyan, J. (1995). *Structure*, **3**, 215–226.

Xu, W., Harrison, S. C. & Eck, M. J. (1997). *Nature (London)*, **385**, 595–602.